01 Jan 1986

Electrodeposition And Analysis Of Tin Selenide Films

R. D. Engelken

Jack L. Boone
Missouri University of Science and Technology

A. Shahnazary

Electrodeposition and Analysis of Tin Selenide Films

$$b = (\partial E_{CORR}/\partial \log C_{O_2})_\omega = 2(\partial E_{CORR}/\partial \log \omega)_{C_{O_2}} \quad [4]$$

Thus, the measured quantities in the open-circuit method are related to and can be used to determine the kinetically significant Tafel slope.

A further important point, which has already been noted earlier (4), is that, since reduction occurs at the limiting rate, the concentration of the reducible species at the electrode surface (molecular oxygen in the present experiment) is essentially zero. Thus, the nature of the reducible species cannot have a significant effect on the kinetics of anodic dissolution, unless it is irreversibly adsorbed on the surface.

It should be possible to apply this technique to the study of metal dissolution and possibly other electrochemical reactions in nonaqueous media, in which reliable kinetic data could so far not be obtained due to excessively high solution resistance combined with relatively high exchange current densities (10).

Acknowledgments

The authors wish to thank Suzanne Reichard for help provided in preparing polarization graphs and figures.

Manuscript submitted Aug. 5, 1985; revised manuscript received Oct. 1, 1985.

The Johns Hopkins University assisted in meeting the publication costs of this article.

REFERENCES

1. F. LaQue, "Marine Corrosion," pp. 141-145, John Wiley & Sons, New York (1975).
2. R. H. Hausler, *Corrosion*, **33**, 117 (1977).
3. J. Postlethwaite, E. Fradzigbe, and S. Arullah, *ibid.*, **34**, 85 (1978).
4. A. C. Makridis, *This Journal*, **107**, 869 (1960).
5. J. Postlethwaite, "Direct Measurement of the Corrosion Current for Oxygen Reduction Corrosion," Electrochemical Corrosion Testing, ASTM STP 727, F. Mansfield and U. Bertocci, Editors, ASTM 290 (1981).
6. P. Bindra and J. Tweedle, *This Journal*, **130**, 1112 (1983).
7. B. Levich, "Physicochemical Hydrodynamics," Prentice-Hall, Englewood Cliffs, NJ (1962).
8. ASTM Standard D1141-75 substitute Oceanwater, ASTM, Philadelphia, PA (1963).
9. R. E. David, G. L. Horvath, and C. W. Tobias, *Electrochim. Acta*, **12**, 287 (1967).
10. S. Ziegel, E. Peled, and E. Gileadi, *ibid.*, **23**, 363 (1978).

Electrodeposition and Analysis of Tin Selenide Films

R. D. Engelken*

Electronic/Photovoltaic Materials Research Group, Department of Engineering, Arkansas State University, State University (Jonesboro), Arkansas 72467

A. K. Berry

Department of Electrical/Computer Engineering, George Mason University, Fairfax, Virginia 22030

T. P. Van Doren, J. L. Boone, and A. Shahnazary

Department of Electrical Engineering, University of Missouri-Rolla, Rolla, Missouri 65401

Electrodeposition has received recent attention (1-23) as a method to produce semiconductor films, especially metal chalcogenides. Electrodeposition processes have utilized the chalcogen in a positive ($HTeO_2^+$, $SeO_3^=$, etc.), negative [$S_x^=$, $WSe_4^=$, etc. (3)], or zero (S_8, $SeSO_3^=$, etc.) valence state.

This note describes the cathodic electrodeposition of tin selenide ($Sn_{1\pm x}Se$) films from acidic aqueous solutions of $SnCl_2$ and SeO_2 or H_2SeO_3 and N,N-dimethylformamide solutions of $SnCl_2$ and dissolved gray selenium. The films range from amorphous to polycrystalline, and measurements indicate an indirect or nondirect bandgap in the range 0.85-0.95 eV.

Experimental Apparatus and Procedure

In the first electrodeposition procedure, the SnSe films were deposited from solutions ($pH \simeq 3$) containing deionized water, HCl, SeO_2 (or H_2SeO_3), and $SnCl_2$. Tin or graphite served as the anode and the $H_2O/HCl/SnCl_2$ solution was electrolytically purified prior to use. All reagents were Alfa or Fisher brand. The PPG indium tin oxide (ITO) and tin oxide (TO)-coated glass substrates (1 in.^{2}) were scrubbed with a test tube brush and detergent and extensively rinsed with deionized water before insertion into a graphite clamp held in place by a polypropylene beaker cover supporting Fisher temperature, pH, and saturated calomel (SCE) reference electrodes. The beaker was positioned on a stirring hot plate with bath temperatures from 20° to 90°C.

Voltammetric sweeps determined that the reversible potential of tin in the solution was approximately −0.4V (SCE) and the cathode voltage was set at −0.35 to −0.4V so that tin could underpotential deposit only through its reaction with selenium. SeO_2 or H_2SeO_3 was added either as a few drops of dilute ($< 10^{-3}M$) aqueous solution or a grain at a time. The selenium salts were immediately reduced to brick-red amorphous selenium by the Sn(II) ions and the solution transformed from a clear to a brick-red color. The current density surged to approximately 20 $\mu A/cm^2$ for several seconds and then rapidly decreased to nearly zero as the H_2SeO_3 and/or $HSeO_3^-$ in the solution was reduced to suspended selenium.

After approximately five such selenium salt additions, the bath color slowly changed from brick-red to yellow-brown, indicating the transformation of red selenium to Sn_xSe suspended in solution. After the color change, the current density could be maintained at 6-30 $\mu A/cm^2$ and many brown to gray $Sn_{1\pm x}$ Se films could be electrodeposited before selenium replenishment was required.

The second electrodeposition technique is similar to the method first described by Baranski and Fawcett (11) and by Roe, Wehzhao, and Gerischer (14). $SnCl_2$ was dissolved in ionic form yielding 0.1-1.0M solutions but the selenium (100-500 mg in 150-250 ml of solvent) dissolved molecularly into Se_x species after the solvent was heated above 120°C. The solution turned a faint yellow-green color upon dissolution of the selenium, possibly indicating the formation of Se_8^{++} and Se_4^{++} ions (24). No suspension or precipitate formation was noted, and there was never any indication of selenium electrodepositing in the elemental state. The bath temperature ranged from 110°-130°C.

Voltammetric analyses on $SnCl_2$-DMF solutions again indicated reversible potentials near −0.4V, and the electrodeposition of SnSe was conducted with cathode volt-

* Electrochemical Society Active Member

ages of −0.4 to −0.5V, just slightly negative of the potential required to plate elemental tin. The SnSe films were produced by the plating of tin at current densities near 30 $\mu A/cm^2$ and its subsequent reaction with the dissolved molecular selenium in the Helmholtz layer and possibly, to a lesser degree, by the reduction of the selenium molecules to divalent $Se_x^=$ species which precipitated with the Sn^{++} on the substrate surface. However, this latter reaction could occur at −0.4 to −0.5V only because of the vanishing $Se_x^=$ activity provided by precipitation with Sn^{++}. Temperatures below 100°C and current densities above 50 $\mu A/cm^2$ resulted in visually tin-rich deposits.

Results and Discussion

The cathode deposits obtained by the process utilizing selenium salts were smooth, uniform, very adherent, and definitely electrodeposits rather than the adsorbed brown Sn_xSe suspension formed in the solution. The film colors ranged from reddish-brown when the films were very thin, to yellow-brown for thicker yet transparent films, to gray when opaque. The thickest films exhibited a grainy appearance and occasionally became covered with loosely adherent gray powder, probably indicative of selenium formed near the cathode from the reduction of Se(IV) by H_2Se produced from the six electron reduction of Se(IV) (21, 22).

Since the deposition voltage was positive of the elemental tin reversible potential, the tin plated only because of the reduction in its activity in the SnSe deposit due to compound formation between it and the plated selenium and/or because of its precipitation with H_2Se, $SnSe_2^=$, or $SnSe_3^=$ (25) produced by selenium reduction.

Open-circuit potential *vs.* time measurements (Quasi-Rest Potential, QRP) (5, 6, 16, 23) indicated a rapid increase from the deposition voltage to values between −0.2 and −0.3V (SCE) in less than a second and a slow increase to values between −0.1 and −0.2V after a minute. The latter values are slightly more positive than the SnSe equilibrium rest potential calculated to be −0.19V from equilibrium considerations (6, 23) for a solution at 25°C, 0.1*M* in Sn^{++}, with a *p*H of 3, and with a $HSeO_3^-$ activity of $3 \cdot 10^{-40}$, as is required for stoichiometric equilibrium between the SnSe and electrolyte. The measured equilibrium rest potentials between −0.1 and −0.2V are consistent with a much higher and physically attainable selenium ion activity and a selenium-rich equilibrium deposit.

The films exhibited weak photocurrents during deposition. When illuminated with a 1000W white light source through a 1-2 in. electrolyte path, cathodic photocurrents of 1.5-9 $\mu A/cm^2$ were observed above a dark current density of 6-30 $\mu A/cm^2$, after a transient photocapacitive spike.

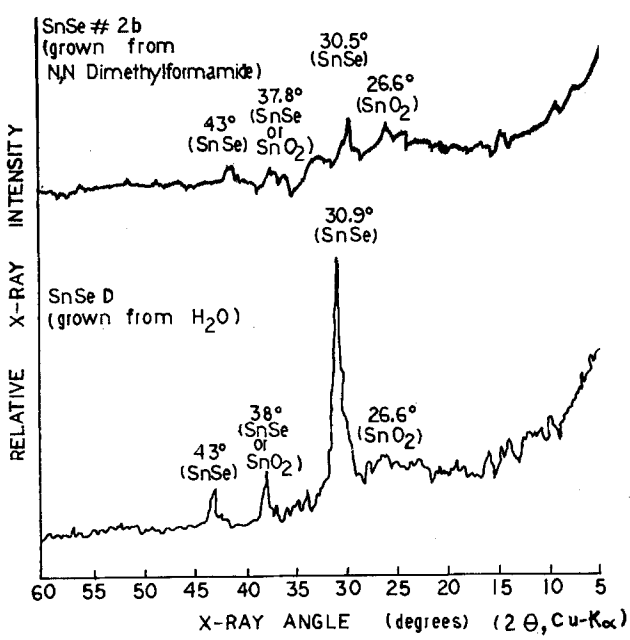

Fig. 1. X-ray diffraction spectra typical of the more polycrystalline electrodeposited $Sn_{1\pm x}Se$ films.

Table I. Tabular microanalysis data for Sample D ($Sn_{0.91}Se$) electrodeposited from aqueous solution

Semi-quantitative analysis: SnSe Sample D
El Norm. K-Ratio

SN-L 0.51293 + − 0.00150
SE-K 0.48706 + − 0.00376

ZAF Correction 20.00 keV 10.00 Degs.

Iter 3	K	[Z]	[A]	[F]	[ZAF]	Atom.%	Wt.%
SN-L	0.512	1.056	1.202	0.999	1.269	47.70	57.88
SE-K	0.487	0.935	1.039	1.000	0.973	52.30	42.12

Films grown from the DMF solution were nearly identical in appearance to those grown from the aqueous solutions but were slightly more adherent and generally exhibited a more grainy and textured surface.

Material Data

Figure 1 exhibits typical x-ray diffraction spectra for the more polycrystalline $Sn_{1\pm x}Se$ films. Numbers and lower case letters (1a, 2b, etc.) were used for labeling those films grown in DMF, and letters (D, E, F, etc.) for those grown in H_2O; the labels have no correlation with stoichiometry. The dominant peak near 30° (Cu-Kα, 2θ) is probably indicative of the SnSe (111) plane and the peaks near 43° and 38° are also indicative of SnSe. However, many films grown by both techniques were amorphous with no x-ray structure.

Because of the presence of tin in the ITO and TO structure coatings, portions of the SnSe films were peeled from the substrate by applying epoxy to a microscope slide and pressing this onto the SnSe film. After drying, the two pieces were pulled apart, thus transferring very small portions of the SnSe film onto the microscope slide and leaving the ITO undisturbed, as verified by resistance measurements. X-ray microprobe analyses indicated a tin atomic percentage between 52% and 47% for films deposited by both techniques, with trace amounts of chlorine and silicon (from the glass) occasionally evident. Thus, the as-deposited films are tin(II) selenide, $Sn_{1\pm x}Se$. Table I exhibits microprobe analysis data for Sample D, grown from aqueous solution and with approximate composition $Sn_{0.91}Se$.

Figure 2 exhibits optical absorbance spectra as measured on a Perkin Elmer-Hitachi 330 spectrophotometer and corrected for substrate absorbance. A moderately strong absorption edge is evident at wavelengths less than 1000 nm. Figure 3 shows data from Fig. 2 plotted as $[h\nu\ (A\text{-}A_0)[^{0.5}$ *vs.* $h\nu$, where $h\nu$ is the photon energy, A is the optical absorbance, and A_0 is a background absorbance due to reflectance, imperfect substrate compensation, impurity absorbance, etc. This plot corresponds to

$$A = A_0 + \frac{(E - E_g)^2}{E}$$

where E_g is the bandgap. This equation should apply to materials exhibiting indirect transitions, or nondirect transitions as occur in amorphous materials with "smeared" bandedges. The plots are reasonably linear and when extrapolated to zero absorbance, yield bandgap values between 0.85 and 0.95 eV. Plots of $[h\nu\ (A\text{-}A_0)]^2$ *vs.* $h\nu$, as correspond to direct transitions, showed no consistent pattern and unreasonably high bandgaps. Thus, SnSe is probably an indirect bandgap material.

Mitchell (29) reported that SnSe single crystals grown by chemical vapor deposition were always p-type and exhibited optical absorbance "cutoff energies" of 0.90 and 0.86 eV, corresponding to two different polarizations. A direct transition was observed at 1.2 eV. The former values are consistent with our measurements and other

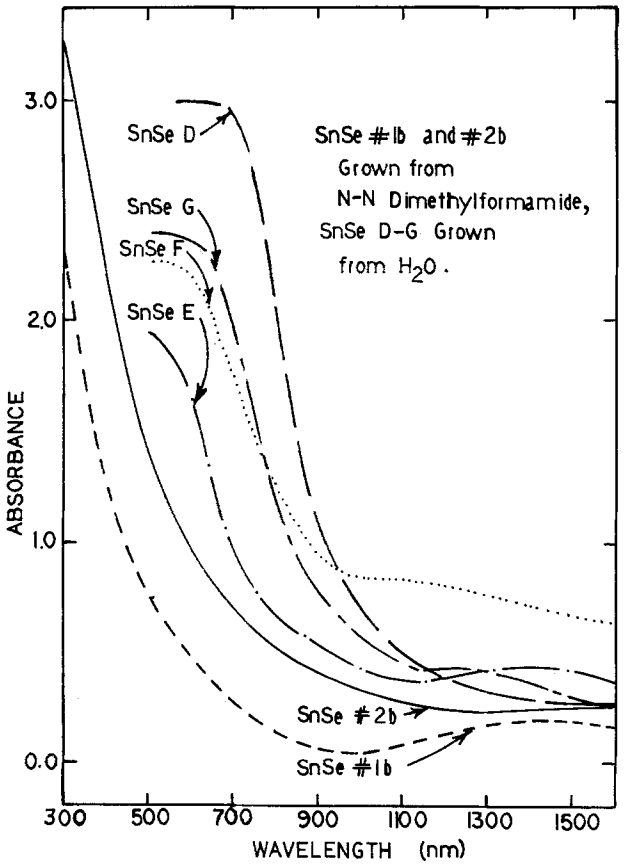

Fig. 2. Optical absorbance spectra for electrodeposited $Sn_{1\pm x}Se$ films

values from 0.89 to 0.93 eV, as reviewed in Ref. (26) and (30).

Annealing amorphous and polycrystalline films in a vacuum at 300°C for several hours had the surprising effect of, in all cases, erasing rather than increasing the x-ray diffraction peak structure. Furthermore, the films were more orange, more transparent, and thinner after annealing with the apparent bandgaps shifting to near 1.3 eV. Microprobe analysis data for annealed films peeled from the substrates indicated a slight decrease in the Sn:Se ratio in the films with the tin percentage varying from 40% to 45%.

The low temperature (≃ 300°C) annealing probably both volatilized the amorphous selenium-rich outer layers, common on films grown from H_2O, and drove selenium into the underlying Sn_xSe layers, thus making the deposits slightly more transparent and orange. Recall that loosely adherent gray selenium powder often formed on the deposit surface because of the reactions

$$Se(IV) + 6e = Se(-II)$$

$$2Se(-II) + Se(IV) = 3Se$$

and because the reference-cathode voltage decreased with thickness, due to large deposit resistivities, and reduced j_{Sn}/j_{Se}, where j is current density. The selenium driven into the microanalyzed layers near the substrate/deposit interface probably decreased the long-range periodicity of the lattice, thus erasing the diffraction structure.

Because tin has a higher melting point (232°C) and boiling point (2260°C) (and, hence, a lower vapor pressure) than selenium (mp = 217°C, bp = 685°C) and because SnSe is much more stable than $SnSe_2$ and the metastable Sn_2Se_3 (mp_{SnSe} ≃ 870°C, mp_{SnSe_2,Sn_2Se_3} ≃ 650°C, and Ref. (30) states that $SnSe_2$ "easily decomposes on heating separating selenium"), it is unlikely that significant tin left the films unless present in local metallic regions in films grown from DMF. In this case, the partial vacuum of the furnace could have evaporated molten tin regions and, again, left a slightly thinner compound deposit. However, optical absorbance, resistivity, x-ray diffraction, and microanalysis data did not indicate significant tin richness for films grown above 100°C from DMF. The amorphous nature of the remaining compound is difficult to explain in this case.

Figure 4 exhibits optical absorbance spectra for Sample N, both before and after annealing. The spectrum of the annealed film has been shifted toward shorter wavelengths and exhibits a smaller sub-bandgap absorbance.

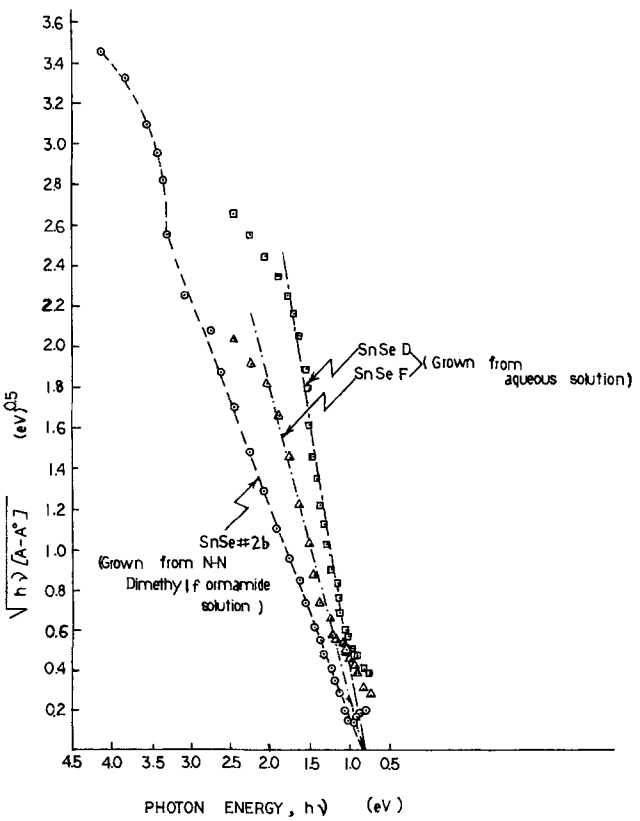

Fig. 3. Plots of $[h\nu(A-A_o)]^{0.5}$ vs. $h\nu$ for the data of Fig. 2. The intercepts of the extrapolated linear regions with the photon energy axis yield indirect or nondirect bandgap estimates between 0.85 and 0.95 eV.

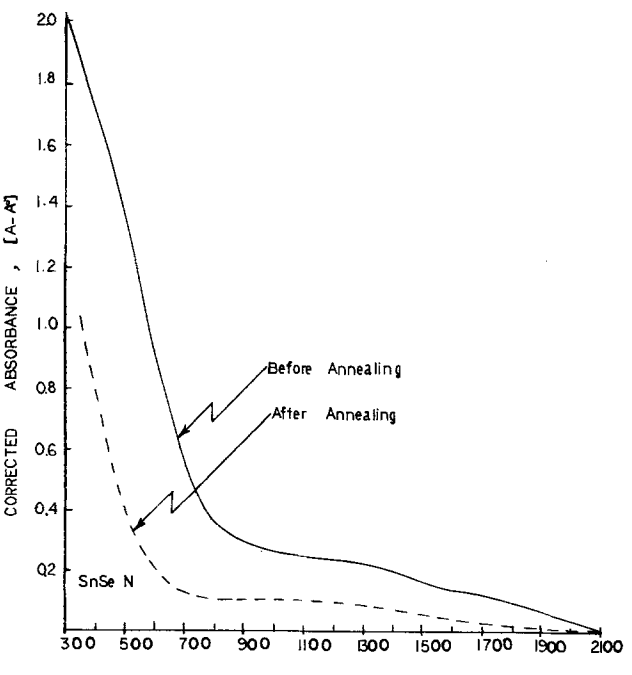

Fig. 4. Optical absorbance spectra for Sample N before and after annealing.

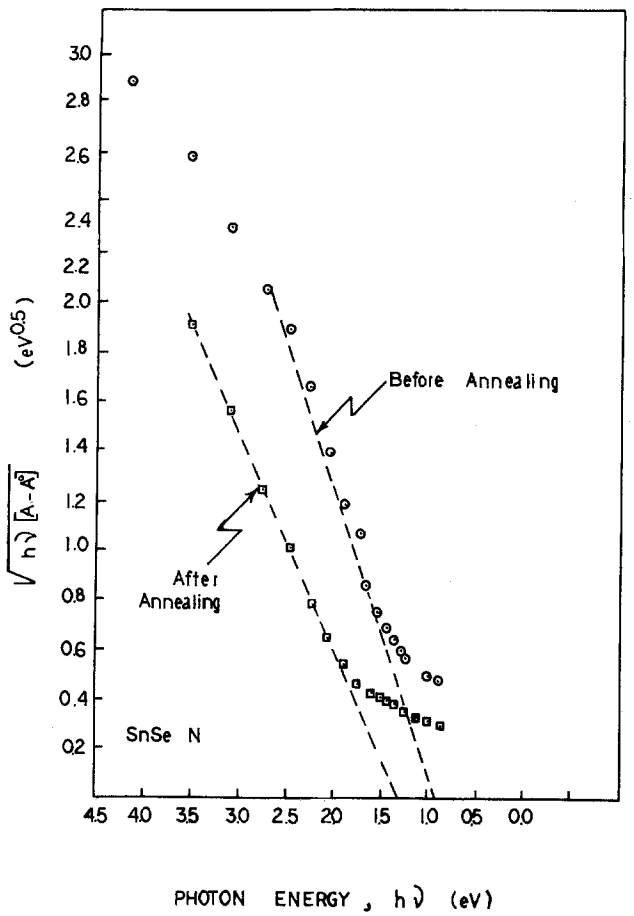

Fig. 5. Plots of $[h\nu(A\text{-}A_0)]^{0.5}$ *vs.* $h\nu$ for the data of Fig. 4. These plots indicate that the apparent bandgap shifts from 0.95 to 1.30 eV after annealing.

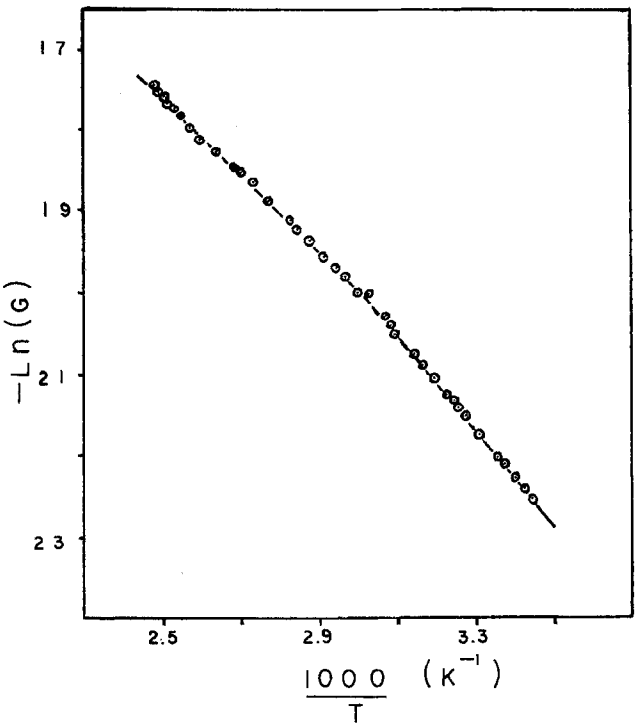

Fig. 6. Semilogarithmic plot of dark conductance *vs.* reciprocal temperature data for a small irregular flake of Sample D peeled from the ITO substrate. The two linear regions suggest activation energies of 0.44 and 0.51 eV for the high and low temperature regions, respectively.

Figure 5 exhibits $[h\nu\ (A\text{-}A_0)]^{0.5}$ plotted *vs.* $h\nu$ for this sample, and the plots are again reasonably linear. From the intercepts of the extrapolated lines with the horizontal axis, it appears that $E_g \simeq 0.95$ eV before annealing and $E_g \simeq 1.30$ eV after annealing.

Gupta, Agarwal, and Srivastava (31) report that SnSe has an indirect bandgap of 1.16 eV at 273°C. Lee, Said, Davis, and Lim (28) report an indirect bandgap of 1.09 eV, and Domingo, Itoga, and Kanneworf (27) report a 0.97 eV indirect bandgap. Our 1.3 eV value is in the vicinity of these single-crystal values and could be slightly greater due to the amorphous nature of the films, even though amorphous materials generally exhibit decreased bandgaps due to "band tailing." However, in some cases (*e.g.*, a-Si) increased gaps are observed. More likely is the presence of some oxygen in the annealed films due to the only partial vacuum. Reference (30) reports compounds such as $Sn_5Se_6O_{22} \cdot xH_2O$, $Sn(SeO_3)_2$, $SnOSeO_4 \cdot xH_2O$, $SnSeO_4$, and $Sn_5Se_4O_6$; $Sn_5Se_4O_6$ has a bandgap of 1.6 eV. The oxygen would not have been detected by microprobe analysis due to its low atomic weight and could have played some part in decreasing the tin/sulfur atomic ratio with annealing.

Because of the excellent adherence of the films, it was very difficult to obtain flakes large enough for electrical contacting, but two small flakes from Sample D were transferred to glass by the epoxy method previously discussed and contacted with silver ink which was allowed to dry at room temperature before measurements were taken. I-V curves were slightly nonlinear with a positive $d^2(I)$:dV^2 but symmetrical. Hot probe measurements indicated that the films were weakly p-type, consistent with Mitchell's findings (29). A current-temperature measurement on the larger flake with a sample voltage of 100V yielded the plot shown in Fig. 6, in which the temperature of a Cambion thermoelectric cooler/heater was rapidly taken to 125°C, held there for 30 min to allow any changes in the silver-SnSe contact interface to stabilize, and then reduced to near 0°C over a 2h period as data were taken. The ln(*G*)-1000/*T* plot exhibits two linear regions with an activation energy of 0.44 eV for the high temperature region and 0.51 eV for the low temperature region. The former value is near the $E_g/2$ value and probably indicates a deep acceptor level. The increase in the activation energy as time progressed is probably due to an increasing bandgap or change in acceptor level caused by the minor amount of annealing during the measurement period. These values place a 0.88 eV lower limit on the bandgap of Sample D, consistent with Fig. 3.

Both samples exhibited photoconductance. Figure 7 exhibits a typical oscilloscope (R_{in} = 1 MΩ) trace of the voltage taken across a 990 kΩ resistor in series with the larger sample (before any heating) when illuminated with a 500W chopped white light source and connected to a 500V dc voltage source. Apparent decay times were in the 5 ms range, probably indicative of deep trap levels. ΔG and G_{Dark} were approximately $2 \cdot 10^{-10}$ and $4 \cdot 10^{-9}$ Ʊ[$\sigma \simeq 10^{-4}$

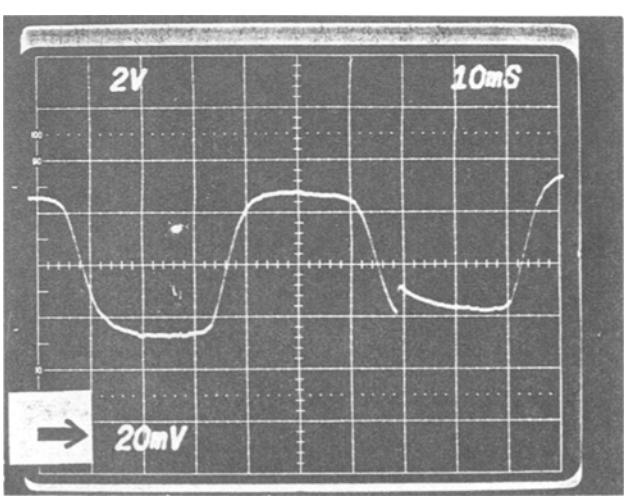

Fig. 7. Room temperature photoconductance signal for the same sample as in Fig. 6. $\Delta G/G \simeq 0.05$ with millisecond decay times.

[Ω-cm]$^{-1}$], respectively, yielding a $\Delta G/G$ value of 0.05. The photoconductance exhibited negligible change as the sample (same as for Fig. 6) was rapidly heated to 125°C but exhibited a slow decrease to one fifth of its initial room temperature value and similar decay times after the 2h cooling period.

Summary

$Sn_{1\pm x}Se$ films have been electrodeposited from aqueous solutions containing $SnCl_2$ and ionically dissolved SeO_2 or H_2SeO_3 and DMF solutions containing $SnCl_2$ and molecularly dissolved selenium powder. The as-deposited films ranged from amorphous to polycrystalline and exhibited indirect or nondirect bandgaps from 0.85 to 0.95 eV. There was little difference between the appearance or material data of the films grown by the two techniques.

Direct reaction between Sn^{++} and H_2SeO_3 or $HSeO_3^-$ in the aqueous solutions yielded a Se/Sn_xSe suspension/precipitate. Although this does not seem to have any serious effect on the deposition process, it does produce a decrease in the concentration and possibly a change in the composition of the ions in solution, as well as preventing *in situ* observation of the deposit and making the cleaning of the apparatus more difficult.

Annealing slightly increased the Se/Sn ratio of microanalyzed layers near the substrate-deposit interface, and erased all x-ray diffraction structure. The bandgaps of the annealed films were shifted from approximately 0.9 eV to approximately 1.30 eV, consistent with the increased Se/Sn ratio.

The films exhibited weak cathodic photocurents during deposition and photoconductance ($\Delta G/G \simeq 0.05$) after deposition. The conductivity of Sample D ($Sn_{0.91}Se$) was estimated to be on the order of 10^{-4} $(\Omega\text{-cm})^{-1}$. Conductance-temperature plots indicated activation energies between 0.44 and 0.51 eV, probably indicative of deep acceptor levels and consistent with the p-type thermal voltage, millisecond photoconductance decay times, and the optical bandgaps.

Acknowledgments

The authors thank the Department of Engineering at Arkansas State University and the Departments of Electrical Engineering at the University of Missouri-Rolla and George Mason University for their support, Betty Minton at ASU and Sherry Engelken for manuscript preparation, and Mike Norberg at UMR for his assistance in the microanalysis measurements.

Manuscript submitted July 19, 1985; revised manuscript received Dec. 2, 1985.

REFERENCES

1. R. D. Engelken and H. E. McCloud, *This Journal*, **132,** 567 (1985).
2. R. D. Engelken and H. E. McCloud, Abstract 429, p. 617, The Electrochemical Society Extended Abstracts, Vol. 84-2, New Orleans, Louisiana, Oct. 7-12, 1984.
3. R. D. Engelken, T. P. Van Doren, J. L. Boone, A. K. Berry, and A. Shahnazary, *Mater. Res. Bull.*, **20,** 1173 (1985).
4. R. D. Engelken, Abstract 430, p. 619, The Electrochemical Society Extended Abstracts, Vol. 84-2, New Orleans, Louisiana, Oct. 7-12, 1984.
5. R. D. Engelken, Abstract 510, p. 723, The Electrochemical Society Extended Abstracts, Vol. 85-1, Toronto, Ontario, Canada, May 12-17, 1985.
6. R. D. Engelken, Ph.D. Thesis, University of Missouri-Rolla (1983).
7. R. D. Engelken and T. P. Van Doren, *This Journal*, **132,** 2904 (1985).
8. R. D. Engelken and T. P. Van Doren, *ibid.*, **132,** 2910 (1985).
9. R. N. Bhattacharya and K. Rajeshwar, *ibid.*, **132,** 732 (1985).
10. E. Fatas, R. Duo, P. Herrasti, F. Arjona, and E. Garcia-Camarero, *ibid.*, **131,** 2243 (1984).
11. A. S. Baranski and W. R. Fawcett, *ibid.*, **127,** 766 (1980).
12. R. N. Bhattacharya, *ibid.*, **130,** 2040 (1983).
13. A. S. Baranski, W. R. Fawcett, A. C. McDonald, R. M. DeNobriga, and J. R. McDonald, *ibid.*, **128,** 963 (1981).
14. D. K. Roe, L. Wehzhao, and H. Gerischer, *J. Electroanal. Chem.*, **136,** 323 (1982).
15. A. S. Baranski and W. R. Fawcett, *This Journal*, **131,** 2508 (1984).
16. M. P. R. Panicker, M. Knaster, and F. A. Kroger, *ibid.*, **125,** 566 (1978).
17. H. J. Gerritsen, *ibid.*, **131,** 136 (1984).
18. G. Fulop, M. Doty, P. Meyers, J. Betz, and C. H. Liu, *Appl. Phys. Lett.*, **40,** 327 (1982).
19. R. N. Bhattacharya, K. Rajeshwar, and R. N. Noufi, *This Journal*, **131,** 939 (1984).
20. M. Takahashi, I. Uosaki, and H. Kita, *ibid.*, **131,** 2305 (1984).
21. M. S. Kazacos and B. Miller, *ibid.*, **127,** 869 (1980).
22. M. S. Kazacos and B. Miller, *ibid.*, **127,** 2378 (1980).
23. F. A. Kroger, *ibid.*, **125,** 2028 (1978).
24. A. F. Troutman-Dickenson, "Comprehensive Inorganic Chemistry-Volume 2" p. 988, Pergamon Press, Oxford (1973).
25. A. F. Troutman-Dickenson, *ibid.*, p. 80.
26. E. G. Bylander, "Materials for Semiconductor Functions," p. 15, Hayden Book Co., New York (1971).
27. G. Domingo, R. S. Itoga, and C. R. Kanneworf, *Phy. Rev. B*, **1143,** 536 (1966).
28. P. A. Lee, G. Said, R. Davis, and T. H. Lim, *J. Phys. Chem. Solids*, **30,** 2719 (1969).
29. D. L. Mitchell, Ph.D. Thesis, Syracuse University, Syracuse, NY (1959).
30. Hubert Bitterner, "Gmelin Handbuch der Anorganischen Chemie, Teil C-2, Zinn," pp. 89-123, Springer-Verlag, Berlin (1975).
31. V. P. Gupta, P. Agarwal, A. Gupta, and V. K. Srivastava, *J. Phys. Chem. Solids*, **43,** 291 (1982).